

Basic Stability of the Ka-band Correlation Receiver

NRAO GBT Memo 249

July 5, 2007

A.I. Harris^{a,b}, S.G. Zonak^a, G. Watts^c

^aUniversity of Maryland; ^bVisiting Scientist, National Radio Astronomy Observatory;

^cNational Radio Astronomy Observatory, Green Bank

ABSTRACT

The basic stability of the Ka-band correlation receiver's active electronics, measured with its inputs terminated at cryogenic temperature, is quite good. Most samples show an Allan variance minimum times are beyond 100 seconds for almost all Zspectrometer lags. The electronic stability is probably dominated by relatively long-term thermal drifts in the receiver's cryogenic or warm IF electronics. Zspectrometer correlator internal offsets have low variance and are very stable. Although low-level ground loops are apparent, we see no sign of pickup on amplifier bias lines. The cross-correlation function offsets we have analyzed earlier are symptoms of gain imbalance rather than a cause of the instability: gain imbalance in the receiver's circuitry before the input hybrid degrades the correlation receiver's rejection of common-mode input signals, including emission from the atmosphere. Rapid nodding and excellent input circuit gain balance are consequently more important for ground-based than space-based correlation receivers.

1 INTRODUCTION

These notes cover the second half of our investigation into the Ka-band receiver's stability. In the first note [1] we discussed the receiver offsets; here we summarize measurements of the gain stability of the system from the input hybrid through the Zspectrometer. This covers all of the cryogenic and room-temperature active electronics.

We made our measurements from June 18 through 21, 2007, with the Ka-band receiver and Zspectrometer in the Green Bank lab. The inputs to the receiver were waveguide loads at the input hybrid. The receiver's cryocooler was running, and the receiver was at its nominal operating temperatures, about 15 K for the front-end components. Some of the room-temperature electronics' thermal shielding was in place for the tests, but one side of the receiver electronics was completely open (Figure 12 in the appendix contains a photograph of the receiver).

2 RESULTS

2.1 Stability tests

The overall receiver and spectrometer gain stability is quite good. Different lags have different minimum times in their Allan variance time [2, 3, 4]. The shortest was 64 seconds, but almost all have minimum times beyond 100 seconds. Even with the receiver input terminated, mismatches cause a small amount of structure across the cross-correlation function (CCF). Figure 1 shows a typical CCF¹, with structure from input reflections prominent near lags 240–250 in the larger-amplitude blue curve. Structure at higher lags (lags to the left in the Figure) is also moderately strong and is most likely due to IF amplifier gain modulation from ground loops, as we discuss

¹14019.tpr, 14023.tpr; 6/20/2007

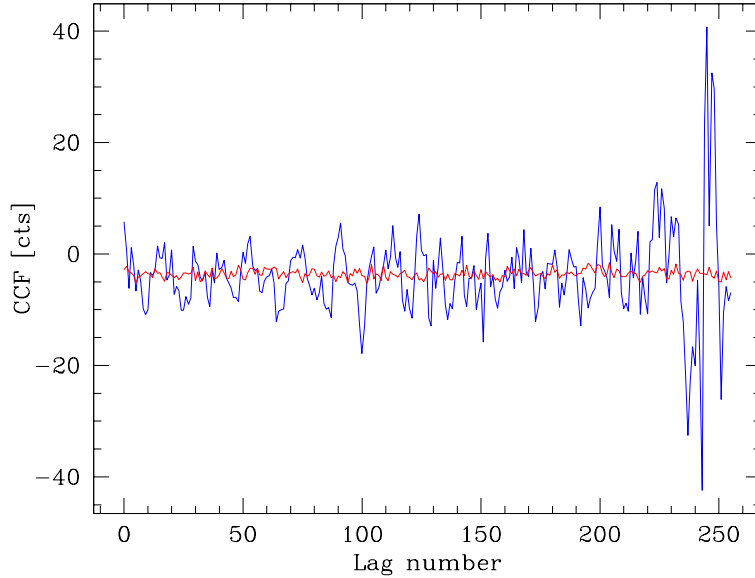


Figure 1: Cross-correlation function from the measurements. Lag decreases to the right, with high time lags at low lag number and the zero (total power) lag near lag 250.

later. Attenuating the IF input to the correlator reduces the lag output amplitudes (red curve in Figure 1), showing that the structure comes through the IF power, and is not a correlator electronics ground loop.

Figures 2 to 4 are typical of the receiver’s time series data² and Allan variance curves for lags across the CCF. Interestingly, the high lags did not have substantially longer Allan variance minimum times than the low lags. As shown in Figures 2 and 3, at all but the near-zero lags, Allan variance minimum times range from of order one hundred to many hundreds of seconds. Longer Allan variance minimum times were correlated with average amplitudes close to -4 counts, the normal correlator offset in the absence of signals. Shorter Allan variance minimum times are associated with lags with the largest absolute value outputs, but there is no general simple correspondence of amplitude and minimum time.

Figures 5 and 6 show data from high-amplitude lags taken at other times than the previous three figures; these may be compared directly with Figure 4. Figure 5 captures some unstable periods, possibly caused by the morning lab startup period. The lags with the largest positive average values had an inverted time-sequence structure compared with nearby lags with large negative values. This indicates that the variation came from an overall gain or offset change rather than a fluctuation in an individual lag’s response. Figure 6 shows a different situation: a warm system with the terminations on the amplifier inputs³, rather than on the input hybrid. The behavior is similar to the cold system’s: a long period of stable output followed by a relatively slow drift.

²tser6_070619, 170/2520; also tser1_070620 170/2520 and tser9_070618 170/2520

³tser3_070531, 384/2520

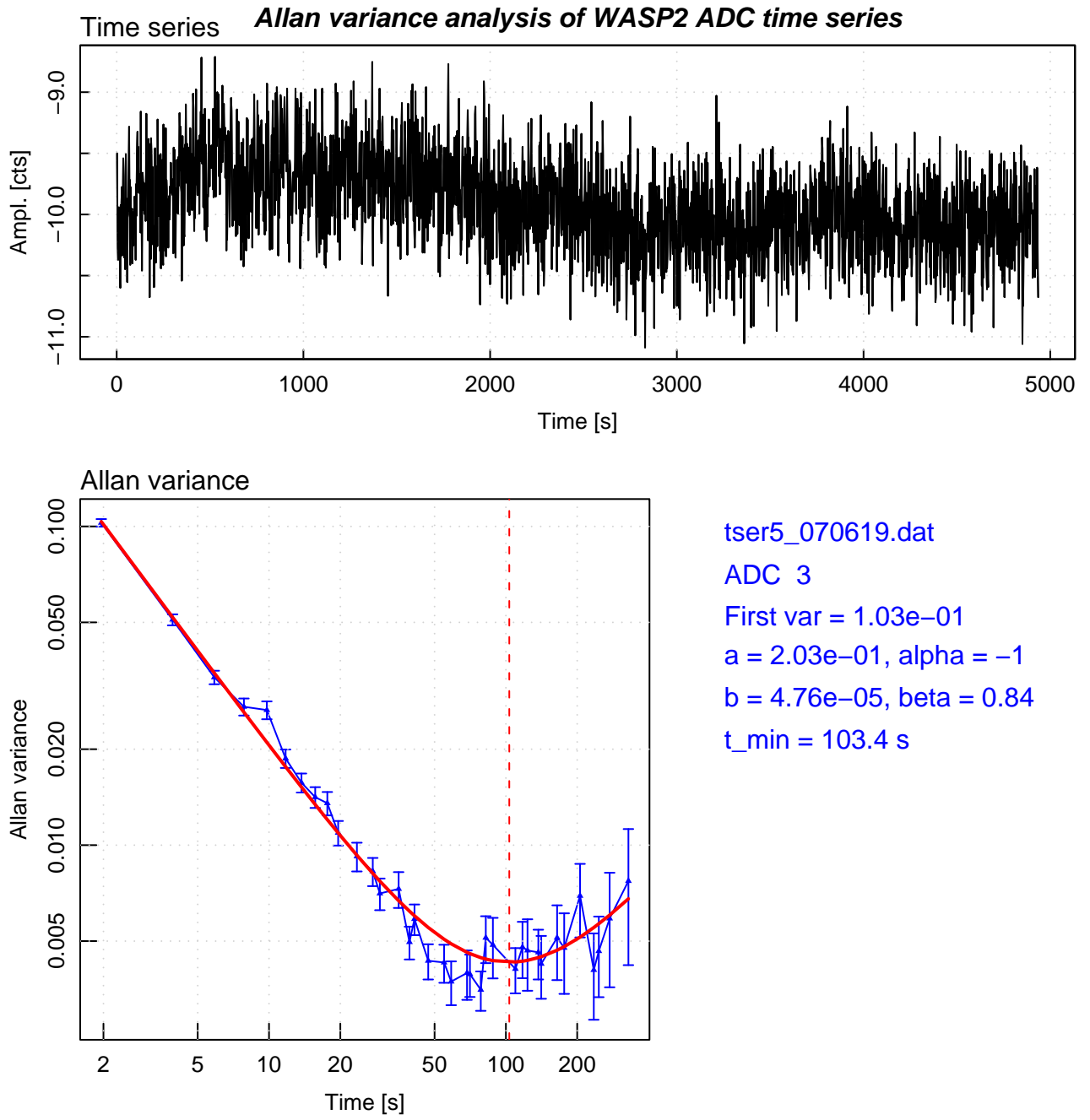


Figure 2: Time series data and Allan variance plot for ADC3

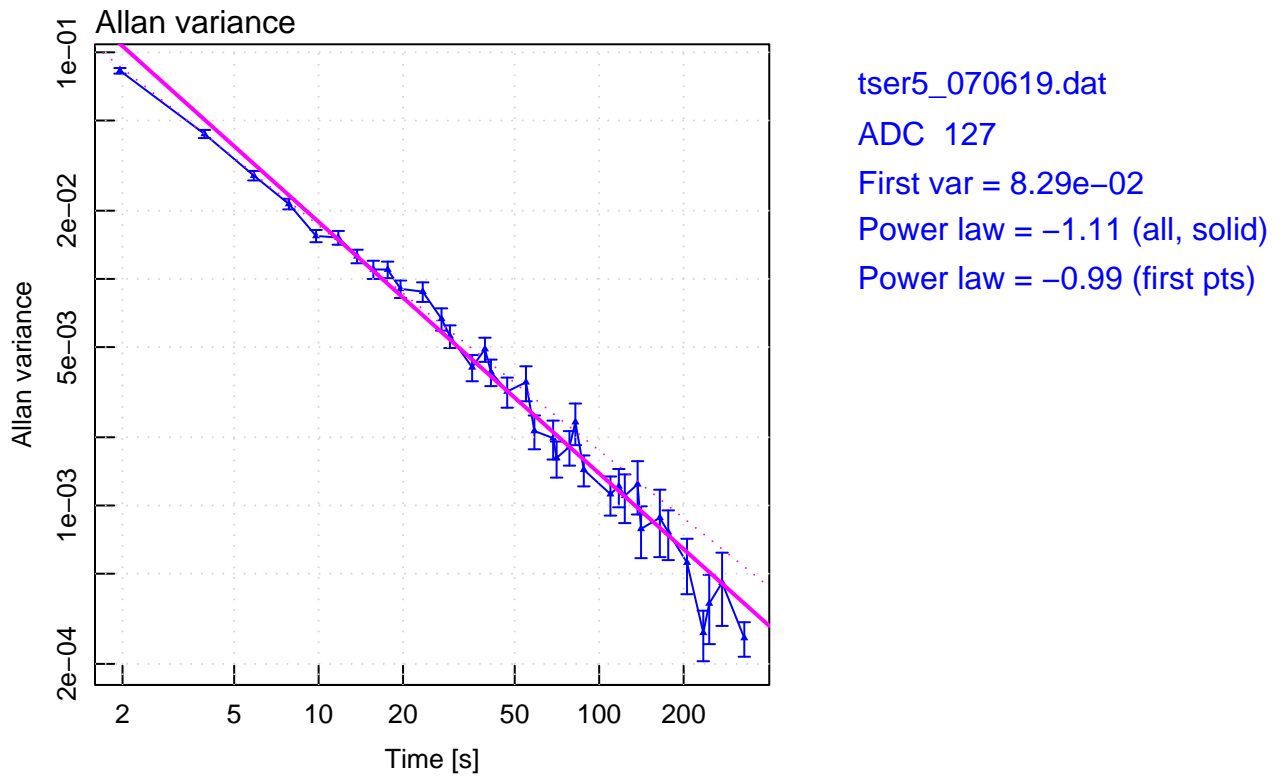
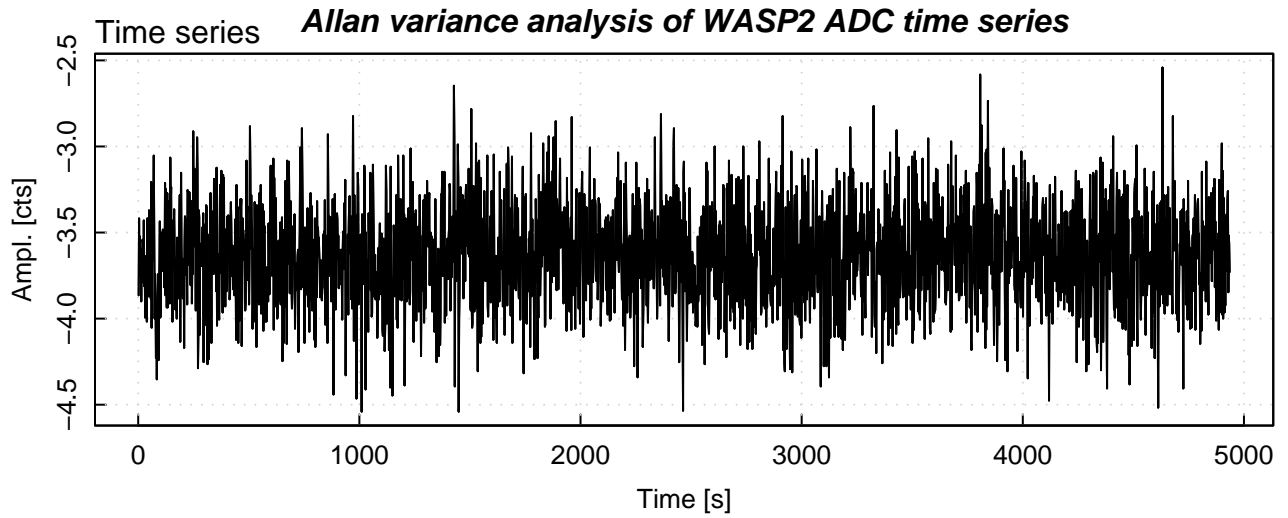


Figure 3: Time series data and Allan variance plot for ADC127

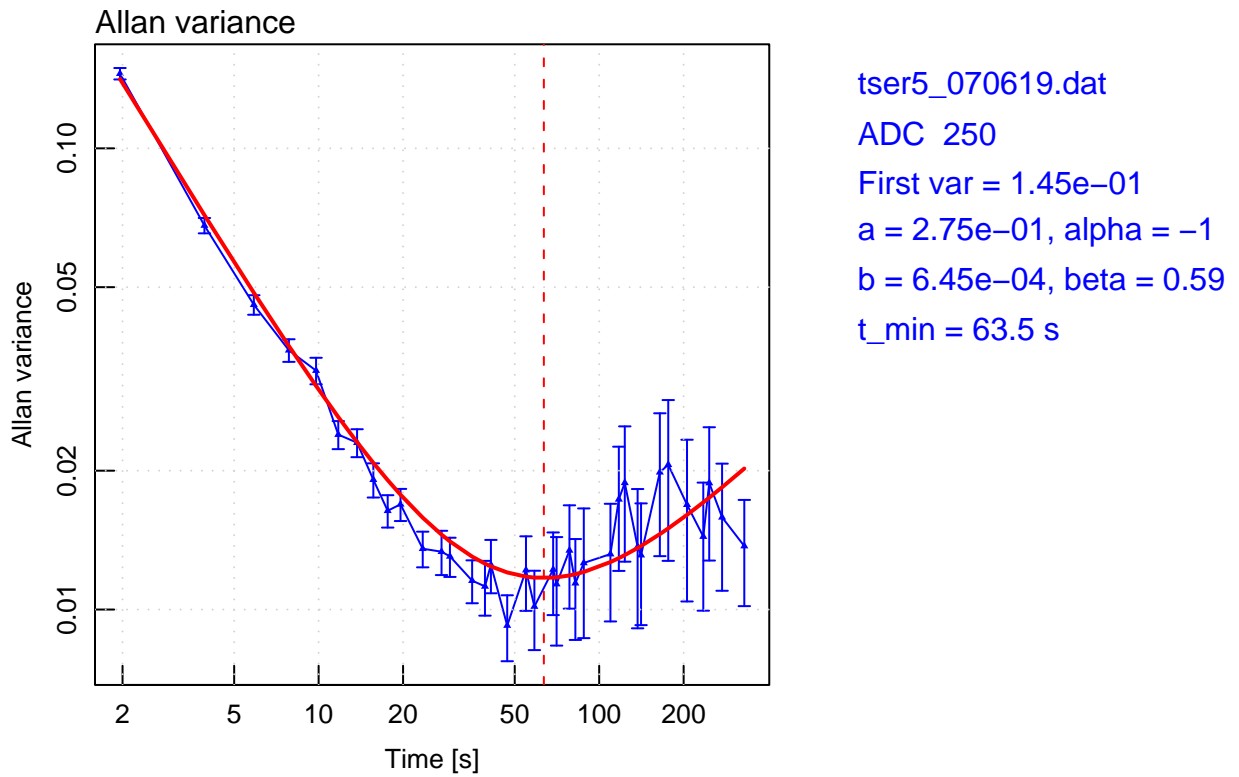
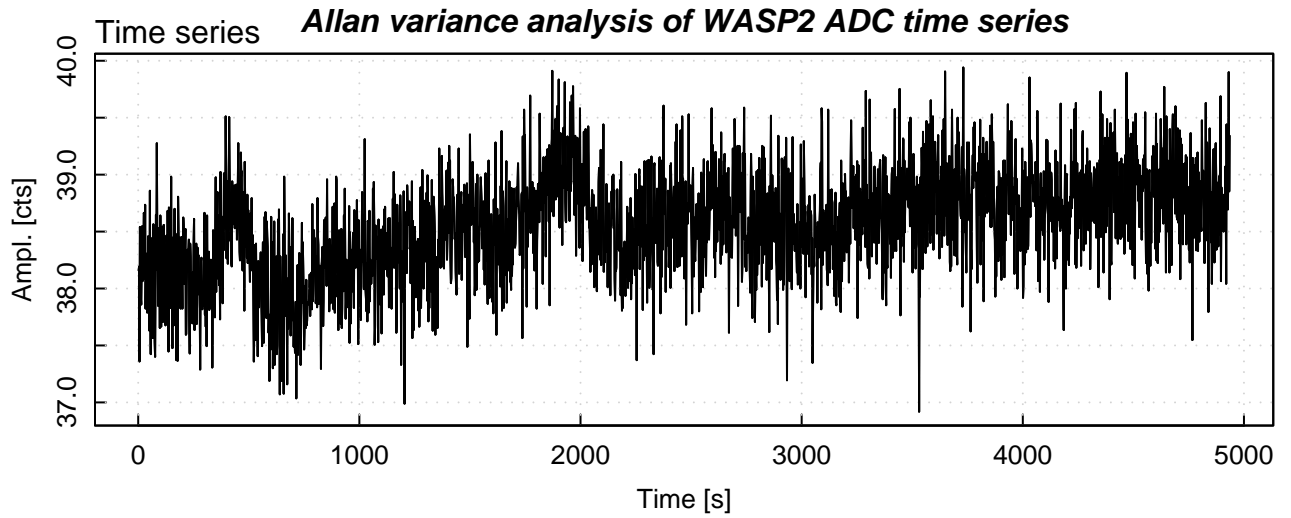


Figure 4: Time series data and Allan variance plot for ADC250

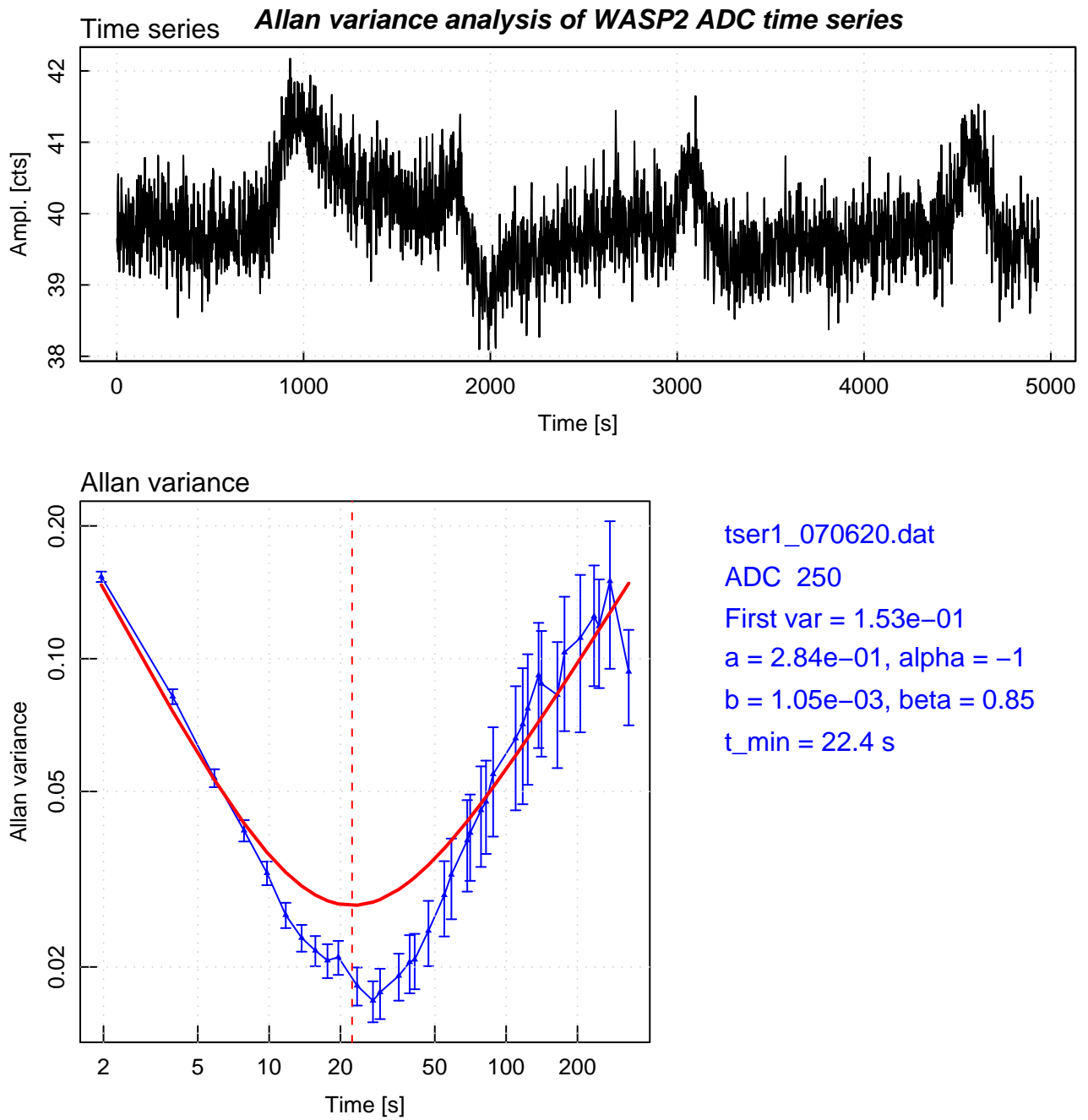


Figure 5: Time series data and Allan variance plot for ADC250 from another run than the previous three figures. Shows rapidly-varying structure.

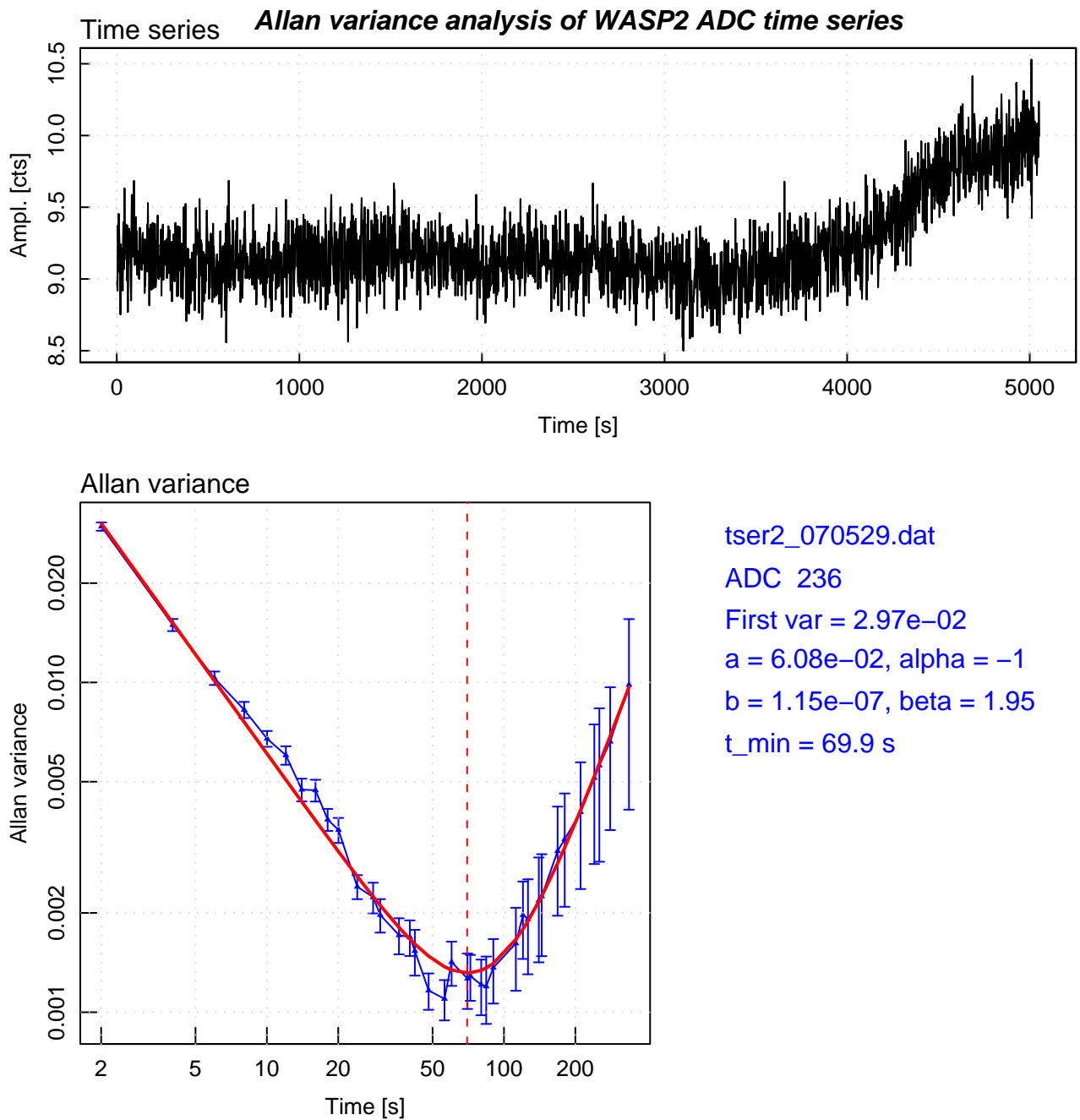


Figure 6: Time series data and Allan variance plot for ADC236 with warm system, terminated amplifier inputs 5/29/2007.

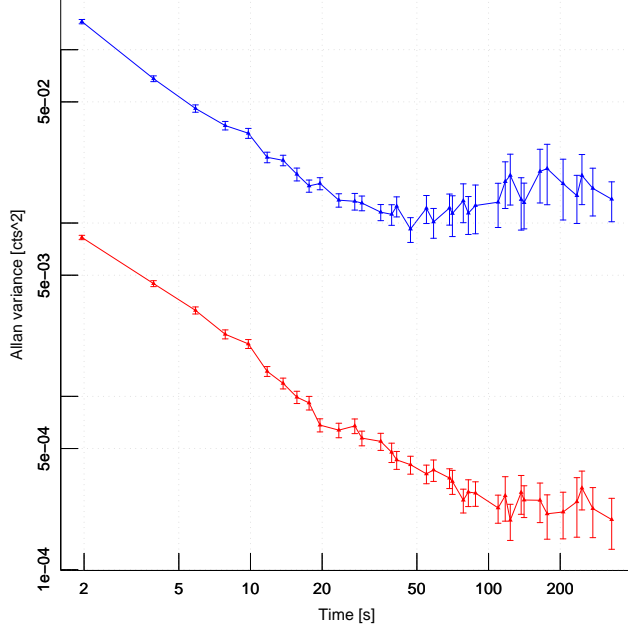


Figure 7: Allan variance plots for ADC 250, with (upper) and without (lower) IF power.

2.2 Offset and pickup tests

The correlator’s intrinsic offsets are small and very stable. Figure 7 is a comparison of Allan variances with and without IF power on the correlator⁴. Radiometric noise should dominate backend noise to keep the backend from degrading the system sensitivity, so the system attenuation is set so the correlator’s variance is an order of magnitude larger with IF power applied⁵ than with no IF power⁶. Figure 7 also shows that the correlator offset is very stable with time, and the system drift is entirely due to IF power drifts.

As we found before [5], the structure in the CCF may be divided into two components: a general structure across all lags, and additional structure near the zero lag. Changing the phase modulation from a single modulator to running both phase modulators in quadrature had a strong effect on the offsets. Further measurements, shown in Figure 8⁷, confirm this conclusion. The upper curve in the figure is the correlator output with fundamental switching; the lower curve is the output with quadrature switching. The offsets are far smaller in the latter case, and the stability improves from an average value of 50 seconds or so to beyond 100 seconds for the quadrature switching. A 50 second stability time shows that the pickup amplitude is pretty stable in time.

Figure 9, the audio-frequency power spectrum of a detector diode connected to one of the receiver’s IF outputs (Σ). Figure 9 is a difference spectrum with the IF on and off⁸ to subtract pickup; noise in the difference accounts for the negative spikes in the spectrum. The SRS model SR770 spectrum analyzer’s internal noise probably sets the noise floor in this measurement, but $1/f$ noise in the receiver IF is visible to about 10 kHz. Phase switching at 5.2 kHz produces

⁴tser5_070619 with IF, tser3_070620 without

⁵See Fig. reffig:adc250

⁶tser3_070620, 170/2520

⁷14033.tpr, 14055.tpr; 6/22/2007

⁸M.dat - K.dat, 6/21/2007

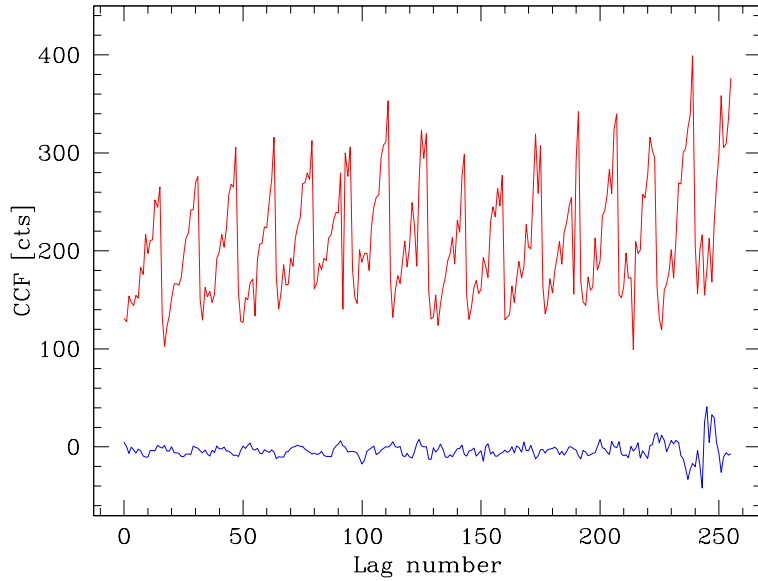


Figure 8: Cross-correlation function with fundamental (lower, red) and quadrature (half-demodulation-frequency; upper, blue) phase switch signals. Lag decreases to the right, with high time lags at low lag number and the zero (total power) lag near lag 250.

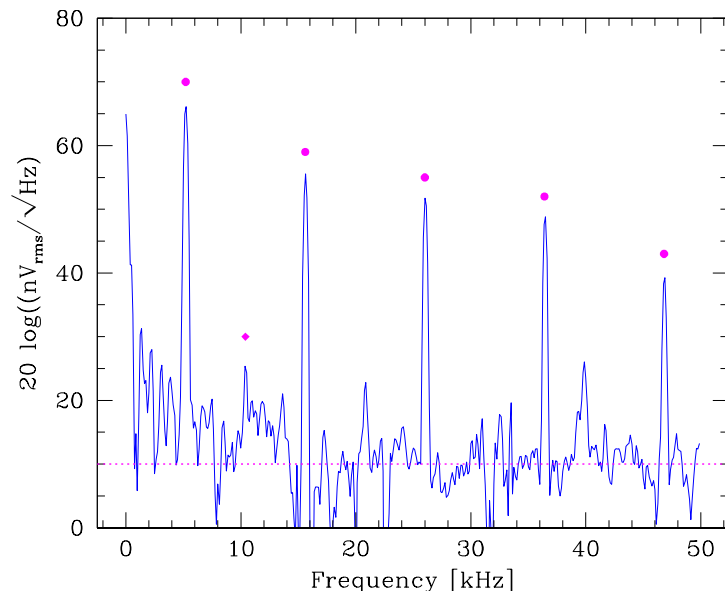


Figure 9: Audio-frequency power spectrum of one of the receiver's IF ports. The 5.2 kHz phase modulation frequency and harmonics are marked with dots; the 10.4 kHz demodulation frequency is marked with a diamond. A dashed line shows the white noise floor level, which is probably set by the spectrum analyzer's internal noise.

the large spikes across the spectrum. In principle, quadrature phase switching has no signal at the demodulation frequency, which is twice that of the two out-of-phase modulation signals. In practice, small differences in the phase modulators' rise and fall times generate weak even harmonics of the the switching frequency. Trace amounts of the second harmonic component, matching the demodulation at 10.4 kHz and its odd harmonics, are present and presumably responsible for the high-lag structure shown in Figure 1. At very low frequencies, we found no clear sign of IF power fluctuations at the cryocooler's 1.2 Hz frequency or harmonics.

We searched for, but did not find, any signs of electric field pickup on the cryogenic amplifier unshielded twisted pair bias lines⁹. We used a SRS model SR850 lock-in amplifier, with the input connected to a detector diode on one of the receiver's IF outputs. The excitation source was a long wire driven by the SR850's sine wave output. Coupling between the radiating wire and a couple of feet of wire on the lock-in's input was very easy to find. We found no strong coupling into the IF system, however, at frequencies of 10 and 100 kHz. The strongest induced signals were about $7 \mu V_{rms}$ at 100 kHz with the radiating wire close to chassis components or the refrigerator lines. The pickup signal was proportional to the the amplitude of the source voltage. Switching the cryogenic low noise amplifiers (LNAs) on and off had little effect on the pickup magnitude, implying that the pickup was probably a ground loop that did not reach the LNAs.

3 DISCUSSION

Our main conclusion is that the correlation receiver's basic stability is quite good, indicating that the active electronics are not limiting the time between telescope nods. With the receiver's inputs terminated at the input hybrid, we found typical Allan variance minimum times beyond 100 seconds, although some high-amplitude lags had minima of 60–70 seconds under most conditions. Environmental effects are important, as we saw minimum times down to 20 seconds at times. We were not able to identify the changes that make for better and worse stability, but note that the timescales are more characteristic of thermal than electrical drifts. Allan variance minimum times of 100 seconds would provide reasonable results with a 20–30 second nod time. The zero and a few low lags may have shorter minimum times if some smooth baseline structure is permissible, as is the case for the Zspectrometer's line searches.

A comparison of the correlation receiver stability times with terminated warm amplifiers and with cold terminations on the input hybrid indicates that neither cooling nor the correlation architecture decrease stability. In general, the time sequence of lag outputs was rather stable behavior for up to thousands of seconds, then some more rapid drift. Long drift times suggest thermal drifts of a large object, changes in cryocooler performance, or varying leakage currents rather than thermal or electronic drifts of small objects. Switching the receiver IF's thermoelectric cooler on and off on a 5 minute cycle left no obvious trace in a time series display. Fanning the electronics gently with a large piece of cardboard also had no clear effect. At any time offset the Zspectrometer correlator internal offsets are very small in comparison with system drifts.

The observations we present here contrast strongly with the poor stability we measured on the telescope in Fall 2006. Then, the best minimum times were 8 seconds at high lags, a few seconds at intermediate lags, and pure drift close to the zero lag. This implies that the Fall 2006 stability problems were connected to some combination of the front-end circuit, which had been removed for the present measurements, and with the atmosphere's emission temperature.

⁹6/19/2007

Load temperature fluctuations could easily have been a problem for laboratory tests.

We explore possible contributions by examining a correlator’s lag output u (see [6]):

$$u = K\alpha\beta [G_X (T_X + T_{Xo}) - G_Y (T_Y + T_{Yo})] g_A g_B^* g_M + u_c, \quad (1)$$

where K is a constant of proportionality, α and β are the hybrid voltage transmission coefficients, $T_{X,Y}$ are the input temperatures at the two inputs, $G_{X,Y}$ are the input power gains before the initial hybrid, $T_{Xo,Yo}$ are the receiver input offset temperatures, $g_{A,B}$ are the voltage gains after the initial hybrid, g_M is the correlator multiplier gain, and u_c is the correlator offset. For approximately balanced input temperatures, it is convenient to write $T_X = T_{com}$ and $T_Y = T_{com} + \Delta T_{diff}$, separating the common and differential mode terms, for

$$u = K\alpha\beta G_X \left[T_{com} \left(1 - \frac{G_Y}{G_X} \right) + \Delta T_{diff} \frac{G_Y}{G_X} + \left(T_{Xo} - T_{Yo} \frac{G_Y}{G_X} \right) \right] g_A g_B^* g_M + u_c. \quad (2)$$

Since we find that the stability of the active electronics, $g_A g_B^* g_M$, and the correlator offsets, u_c , are much better than the system stability measured on the telescope in Fall 2006, the dominant instability terms for the overall system lie within the square brackets in equation (2). We discuss each term and speculate on its origin and importance below.

The first term in square brackets represents a residual signal left from input gain imbalance; ideally, $G_X = G_Y$, and the receiver perfectly rejects common-mode signals. When the input gains are not balanced, the output signal depends on fluctuations in the sky temperature T_{com} with a multiplicative factor $(1 - G_Y/G_X)$. Fluctuations in either gain or temperature, G_Y/G_X or T_{com} , affect the correlator’s output.

We expect that gain (or loss) fluctuation timescales are longer than the 6–8 second fluctuation timescales we found on the telescope [5]. The atmospheric losses should be very closely matched since the atmospheric transmission is high and relatively featureless across the Ka band. Differential optical losses should also be small as long as the horns are symmetrically placed about the GBT’s optical axis, especially given the small optical reflections from the GBT’s off-axis design. Inside the receiver, the dominant loss is associated with the orthomode transducers (OMTs) [1]; these are in a stable environment and unlikely to vary rapidly.

Common-mode temperature changes could explain the signal fluctuations we measured on the telescope in Fall 2006. Figures 9 and 10 from the Zspectrometer 2006 Commissioning Report [5], reproduced here as Figures 10 and 11, show peak total power temperature swings of 0.8 K on timescales of 20 seconds and longer. The telescope was parked in its access position for these measurements, with the surface adjusters inactive, on a windy and cloudy day. The crossing time over the 100 m diameter telescope is 22 seconds with a 10 mph (4.5 m/s) wind speed, which is consistent with the fluctuation timescales. A value of $G_Y/G_X \approx 0.9$ [5] would imply common-mode temperature changes of about 8 K, however, which seems large even with clouds overhead. Atmospheric instabilities do provide a natural explanation for changes in stability, apparent by comparing Figures 10 and 11, and the observation that the Caltech Continuum Backend system stability is weather-dependent. (We do not have enough experience with the Zspectrometer system to comment on operation in different weather conditions.) A complicating observation is that we measured substantial fluctuations at the long lags (rapid spectral variation) on the telescope. This would indicate fluctuations in spectral structure that changes on the scale of tens of megahertz, either from changes in the receiver’s passband or in the atmospheric spectrum. Pressure broadens lines within the troposphere to several gigahertz, but narrow lines could conceivably be produced in the stratosphere.

Atmospheric temperature differences along the columns toward the two sky beam positions, or load temperature differences in the laboratory, are indistinguishable from astronomical signals

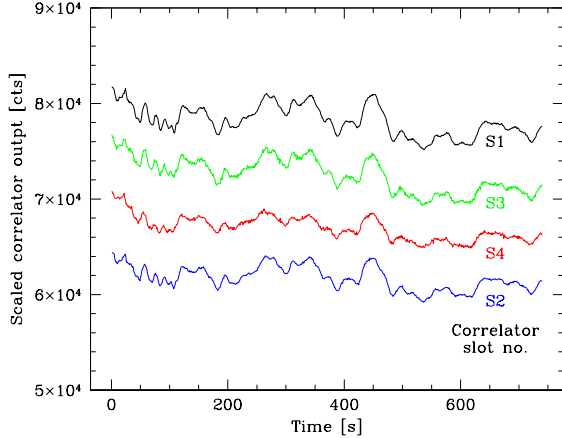


Figure 10: Total power from all correlators versus time for the receiver on the sky and the telescope in its service position in November 2006. Correlator outputs have been scaled and shifted for comparison.

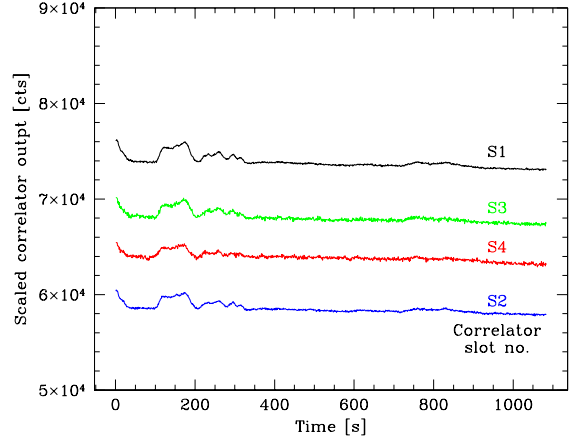


Figure 11: Continuation of time series in Figure 10 after a brief break.

in the differential-mode term proportional to T_{diff} in equation (2). A basic assumption is that the beams overlap well through the fluctuating part of the atmosphere, so the correlation architecture subtracts the common-mode part of the signal. With a $1.8'$ beam separation, the two beams should overlap well through the most emissive part of the atmosphere. At an altitude 6 km above the telescope, a representative altitude above which little tropospheric water vapor is present [7, p. 179], the divergence is 3 m, a small fraction of the beam size. Differences in wide-angle beam patterns for the two horns may be more important than the beam divergence in power differences between the two paths through the atmosphere.

In laboratory measurements, as a number of colleagues have noted, small temperature differences between different parts of the input loads will be important. With the Zspectrometer's lag bandwidth over typical integration time, the radiometer equation gives an approximate differential load stability requirement,

$$\Delta T_{rms} = \frac{20 \text{ K}}{\sqrt{4 \text{ GHz} \times 1 \text{ s}}} = 0.3 \text{ mK} . \quad (3)$$

While this is difficult to reach in the laboratory, it should be attainable by carefully insulating the loads from stray air currents.

Finally, the last term in equation (2)'s square brackets is due to changes in the receiver's internal offset temperatures. These are caused by reflections and loss within the receiver's input waveguide circuit, and are unlikely to change on timescales of a few seconds. Small changes in reflections at the amplifiers' inputs could conceivably affect the amplifier stability or noise temperature by presenting unfavorable source impedances, but we saw no sign of that in the measurements we report here.

4 CONCLUSIONS

Measurements of the Ka band receiver with cryogenic loads at its input shows that the stability of the active electronics in the receiver and Zspectrometer is quite good, with typical Allan

variance minimum times of 100 seconds or longer in almost all lags. This is substantially better than the total system stability on the telescope, which was less than ten seconds even at the longest lags.

Pickup from ground loops is present at low levels but does not dominate the receiver's stability. We were unable to measure pickup on the LNA bias lines to very low levels; it is unlikely that coupling here is a problem for stability.

The disparity in timescales for the receiver terminated on loads in the cryostat and on the sky points to inadequate rejection of atmospheric common-mode input signals as the main cause of the system stability, rather than electronic gain fluctuations multiplying an otherwise relatively stable offset signal. The cross-correlation function offsets we analyzed in [5] and [1] are thus a symptom of gain imbalance rather than a cause of the instability. Sensitivity to common-mode signals is a smaller problem for space-based receivers such as WMAP, which have stable common-mode input signals; this is an important distinction for ground-based systems. Well-matched input circuits, a stable atmosphere, and fast nodding are all important design elements for ground-based correlation receivers.

ACKNOWLEDGMENTS

University of Maryland participation in this work was supported by the National Science Foundation and an NRAO Visitor's Program award to AH.

REFERENCES

- [1] A. Harris, S. Zonak, and G. Watts, "Symmetry in the Ka-band correlation receiver's input circuit and spectral baseline structure." NRAO Green Bank Telescope memo series No. 248, 2007. <http://wiki.gb.nrao.edu/bin/view/Knowledge/GBTMemos>.
- [2] D. W. Allan, "Statistics of atomic frequency standards," *Proc. IEEE*, vol. 54, pp. 221–230, 1966.
- [3] J. Rutman and F. Walls, "Characterization of frequency stability in precision frequency sources," *Proc. IEEE*, vol. 79, pp. 952–960, 1991.
- [4] R. Schieder and C. Kramer, "Optimization of heterodyne observations using Allan variance measurements," *Astron. Astrophys.*, vol. 373, pp. 746–756, 2001.
- [5] A. Harris, S. Zonak, K. Rauch, A. Baker, G. Watts, K. O'Neil, R. Crea-ger, B. Garwood, and P. Marganian, "Zspectrometer commissioning report, Fall 2006." NRAO Green Bank Telescope memo series No. 245, 2007. <http://wiki.gb.nrao.edu/bin/view/Knowledge/GBTMemos>.
- [6] A. Harris, "Spectroscopy with multichannel correlation radiometers," *Rev. Sci. Inst.*, vol. 76, pp. 4503–+, May 2005.
- [7] E. R. Westwater, "Ground-based microwave remote sensing of meteorological variables (chapter 4)," in *Atmospheric Remote Sensing by Microwave Radiometry* (M. A. Janssen, ed.), J.W. Wiley & Sons, 1993.

APPENDIX

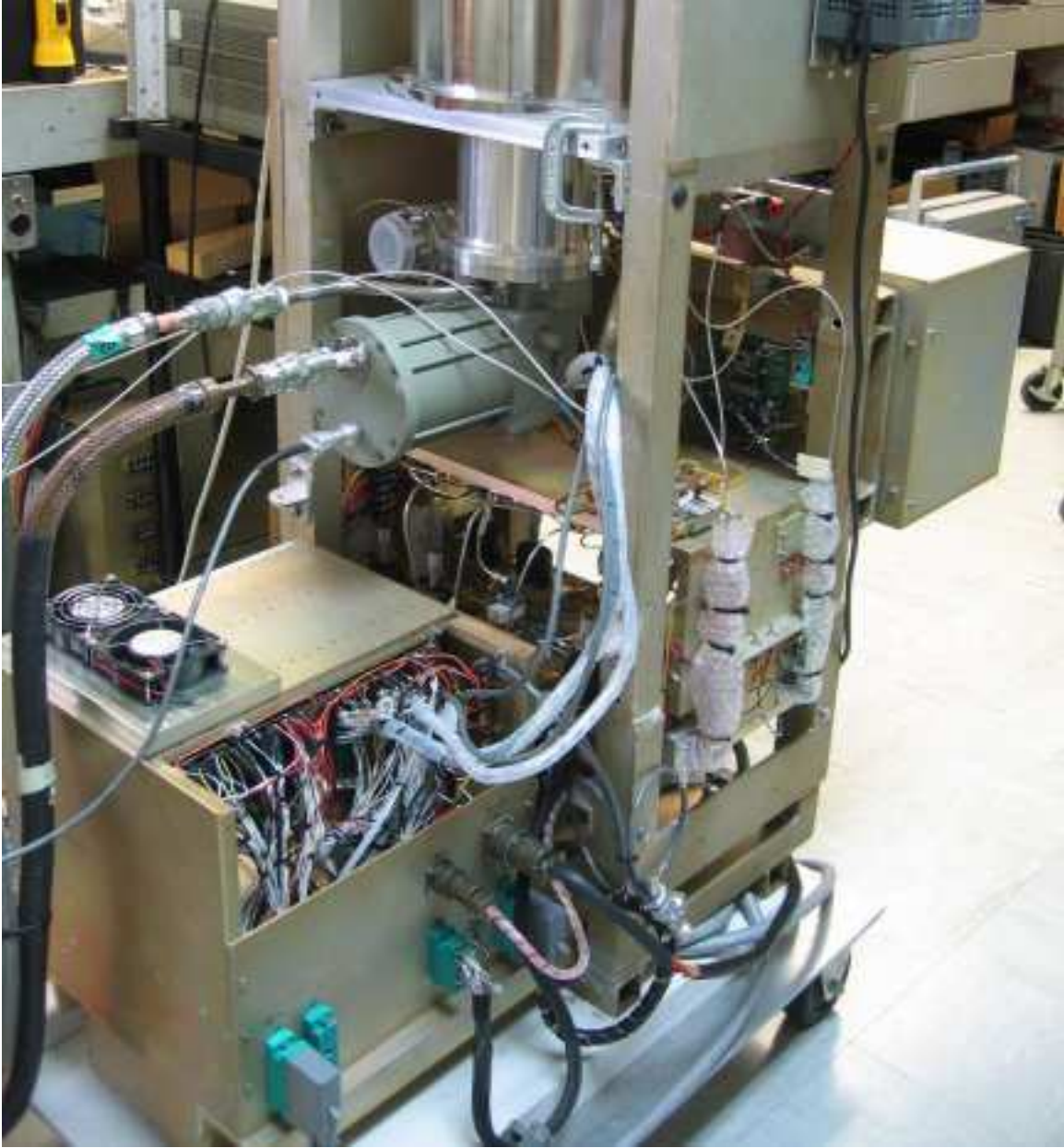


Figure 12: Photograph of the Ka-band receiver's electronics, behind and below the cryostat.